O-GlcNAcylation is a key modulator of skeletal muscle sarcomeric morphometry associated to modulation of protein-protein interactions

Matthias Lambert, Elodie Richard, Sophie Duban-Deweer, Frederic Krzewinski, Barbara Deracinois, Erwan Dupont, Bruno Bastide, Caroline Cieniewski-Bernard

PII: S0304-4165(16)30216-1
DOI: doi: 10.1016/j.bbagen.2016.06.011
Reference: BBAGEN 28523

To appear in: *BBA - General Subjects*

Received date: 14 March 2016
Revised date: 18 May 2016
Accepted date: 6 June 2016

Please cite this article as: Matthias Lambert, Elodie Richard, Sophie Duban-Deweer, Frederic Krzewinski, Barbara Deracinois, Erwan Dupont, Bruno Bastide, Caroline Cieniewski-Bernard, *O*-GlcNAcylation is a key modulator of skeletal muscle sarcomeric morphometry associated to modulation of protein-protein interactions, *BBA - General Subjects* (2016), doi: 10.1016/j.bbagen.2016.06.011

O-GlcNAcylation is a key modulator of skeletal muscle sarcomeric morphometry associated to modulation of protein-protein interactions

Matthias Lambert[1], Elodie Richard[2], Sophie Duban-Deweer[3], Frederic Krzewinski[4], Barbara Deracinois[1], Erwan Dupont[1], Bruno Bastide[1], and Caroline Cieniewski-Bernard[1]

[1]Univ.Lille, EA7369-URePSSS, Unité de Recherche Pluridisciplinaire Sport, Santé, Société, Equipe « Activité Physique, Muscle, Santé », F-59000 Lille, France

[2]BiCeL (BioImaging Center of Lille - Campus Lille 1), Univ.Lille, FR3688 CNRS FRABio, F-59000 Lille, France

[3]Laboratoire de la barrière hémato-encéphalique (LBHE) – EA2465, Université d'Artois, Faculté Jean Perrin, 62307 Lens, France

[4]PAGés (Plateforme d'Analyses des Glycoconjugués), Univ.Lille, CNRS, UMR 8576, UGSF, Unité de Glycobiologie Structurale et Fonctionnelle, F-59000 Lille, France

To whom correspondence should be addressed: Caroline Cieniewski-Bernard, EA7369-URePSSS, Unité de Recherche Pluridisciplinaire Sport, Santé, Société, Equipe « Activité Physique, Muscle, Santé », Université de Lille 1, 59650 Villeneuve d'Ascq, France, Tel: (33)3 20 43 40 89; Fax: (33)3 20 43 68 88; E-mail: caroline.cieniewski-bernard@univ-lille1.fr

ABSTRACT

Background: The sarcomere structure of skeletal muscle is determined through multiple protein-protein interactions within an intricate sarcomeric cytoskeleton network. The molecular

mechanisms involved in the regulation of this sarcomeric organization, essential to muscle function, remain unclear. O-GlcNAcylation, a post-translational modification modifying several key structural proteins and previously described as a modulator of the contractile activity, was never considered to date in the sarcomeric organization.

Methods: C2C12 skeletal myotubes were treated with Thiamet-G (OGA inhibitor) to increase the global O-GlcNAcylation level respectively.

Results: Our data clearly showed a modulation of the O-GlcNAc level more sensitive and dynamic in the myofilament-enriched fraction than total proteome. This fine O-GlcNAc level modulation was closely related to changes of the sarcomeric morphometry. Indeed, the dark-band and M-line widths increased, while the I-band width and the sarcomere length decreased according to the myofilament O-GlcNAc level. Some structural proteins of the sarcomere such as desmin, αB-crystallin, α-actinin, moesin and filamin-C have been identified within modulated protein complexes through O-GlcNAc level variations. Their interactions seemed to be changed, especially for desmin and αB-crystallin.

Conclusions: For the first time, our findings clearly demonstrate that O-GlcNAcylation, through dynamic regulations of the structural interactome, could be an important modulator of the sarcomeric structure and may provide new insights in the understanding of molecular mechanisms of neuromuscular diseases characterized by a disorganization of the sarcomeric structure.

General significance: In the present study, we demonstrated a role of O-GlcNAcylation in the sarcomeric structure modulation.

Keywords: Sarcomere structure, skeletal muscle cells, O-GlcNAcylation, protein-protein interactions, desmin, αB-crystallin

INTRODUCTION

The sarcomere is the functional unit of the skeletal muscle, presenting an accurate striated organization essential for force generation. While contractile and regulatory proteins are the main actors of sarcomere shortening and muscle contraction, structural proteins maintain this highly ordered organization termed sarcomeric structure. These constitutive proteins are closely arranged in various interconnected complexes, leading to an intricate network described nowadays as a "sarcomeric cytoskeleton" [1]. The sarcomeric structure is dynamic [2], combining coordinated changes in structural protein homeostasis [3] as well as in its assembly and maintenance [4]. This dynamism, required for sarcomere equilibrium, is dependent and regulated by kinetic of protein-protein interactions [5] [6], in particular at two nodal points of the sarcomere: the M-line and the Z-line [7]. For instance, phosphorylation is clearly known to be involved in the maintenance of this sarcomeric structure by modulating some protein-protein interactions on myomesin [8], telethonin [9], or desmin [10] [11].

However, while phosphorylation regulates a wide field of the muscle physiology, another post-translational modification that interplays with phosphorylation (for reviews [12] [13] [14]) is important as well. O-linked N-acetyl-glucosaminylation, termed O-GlcNAcylation, is an atypical, reversible and dynamic glycosylation. Occurring exclusively on nucleocytoplasmic and mitochondrial proteins [15] [16] [17], O-GlcNAcylation is mediated by a couple of antagonist enzymes: the OGT (uridine diphospho-N-acetylglucosamine: peptide beta-N-acetyl-glucosaminyl-transferase) transfers the monosaccharide from the donor UDP-GlcNAc to the serine or threonine hydroxyl group of a protein through a beta linkage [18] [19], while OGA (beta-N-acetylglucosaminidase) hydrolyses the O-GlcNAc moieties from O-GlcNAcylated proteins [20]. Like phosphorylation, the O-GlcNAcylation is involved in almost all if not all intracellular processes [14] and its deregulation can play a crucial role in the etiology of several diseases such as type II diabetes [21], cancer [22] [23], neurodegenerative disorders [24] [25], heart [26] [27] and skeletal muscle diseases [28] [29] [30] [31].

Indeed, over the last ten years, more and more accumulated data demonstrate the involvement of O-GlcNAcylation in skeletal muscle physiology (for review [32]). In our lab, it has recently been shown that OGA and OGT are located at the nodal Z-line [33] and many myofibrillar proteins have been identified to be O-GlcNAc modified. Among them, some contractile and regulatory proteins that can be related to the fact that O-GlcNAcylation is a modulator of skeletal muscle contractile activity, in particular on the calcium activation properties [34] [35]. Interestingly, several key structural proteins of the sarcomere are also O-GlcNAcylated, including

αB-crystallin, α-actinin, desmin [36] [37] [35], ZASP [38], filamin-C, myotilin (unpublished data from our lab). Moreover, some studies strongly suggest the involvement of O-GlcNAcylation in protein-protein interactions. Indeed, some O-GlcNAc sites are located close to the interaction domain between myosin, and titin or myomesin, or in polymerization domain on myosin [39]. In this same study, some of the O-GlcNAc sites corresponded to mutated sites closely associated to the development of muscle pathologies such as Laing myopathy [39]. In addition, O-GlcNAcylation seems to play a role in the polymerization state of some intermediate filaments by modulating phosphorylation [40] [41] [11]. Finally, it is noteworthy that desmin presents lectinic properties toward O-GlcNAc moieties [42], which reinforce the role of O-GlcNAc in protein-protein interactions.

However, to date and despite these observations, no scientific evidence shows that O-GlcNAcylation modulates the sarcomere organization. The purpose of this study is to determine whether O-GlcNAcylation could be involved in the regulation of the sarcomeric structure, and in the modulation of its structural interactome. To this aim, we modulated the global O-GlcNAcylation level in C2C12 myotubes through pharmacological treatments to define whether sarcomeric structure could be modulated through the variation of O-GlcNAcylation level. Secondly, we attempted to determine if O-GlcNAcylation variation could modulate the structural interactome in C2C12 myotubes. In the present paper, we identified some structural proteins within the modulated protein complexes, and determined whether their protein-protein interactions have been modulated after variation of global O-GlcNAcylation level, in particular the interaction between desmin and its molecular chaperone, *i.e.* the αB-crystallin.

EXPERIMENTAL PROCEDURES

C2C12 cells culture

Myoblasts proliferation and myotubes differentiation **-** C2C12 mouse myoblasts (ATCC: American Type Culture Collection, Manassas, VA) were grown in proliferation medium (PM), corresponding to Dulbecco's Modified Eagle Medium (DMEM, Gibco) supplemented with 10% foetal calf serum (Gibco) and 1% antibiotics/antimycotics. Cells were plated at a density of $2x10^5$ cells/ml in PM. When reaching 80-90% confluence, myoblasts were induced to differentiate into myotubes by switching the PM to DMEM containing 2% heat-inactivated horse serum (Gibco) and antibiotics/antimycotics (DM, Differentiation Medium). The shifting time to DM was assigned to day 0 of differentiation.

All cultures were performed at 37°C in a 5% CO_2-humidified atmosphere; media were changed every 48 hours, and myotubes formation was monitored daily.

Pharmacological treatments **-** After 5 days of differentiation, myotubes were submitted to pharmacological treatments in order to modulate the global O-GlcNAc level. Thiamet-G (Thiazoline amino-ethyl gluco-configured, Cayman chemicals), stocked in 1M HEPES pH 7.5 (as reported by others [43]), was applied for 4 hours at different concentrations (0.1, 0.5 and 1.0 µM) in DM containing a final concentration of 1 mM HEPES. Thiamet-G treatments had a control corresponding to DM containing HEPES for 4 hours (without pharmacological molecule). Reversion treatments corresponding to post-treatment with DM and HEPES without 0.5 µM of Thiamet-G for 2 and 4 hours were also performed. Agent concentrations and time treatments were determined from the literature [44] and preliminary experiments. All experiments were carried out after treatments on 5-days differentiated myotubes. At this stage of differentiation, C2C12 myotubes were fully differentiated and developed mature sarcomeres.

Immunofluorescence labeling and sarcomeric morphometry **-** C2C12 myoblasts were plated in Lab-Tek chamber slides at a density of $2x10^5$ cells/ml in PM, and then differentiated as described above. Cells were washed three-times with cold PBS (Phosphate-Buffered Saline) and fixed in 4% paraformaldehyde (PFA) in PBS overnight at 4°C. PFA was removed by 3 rinses with PBS and cells were permeabilized in 0.2% Triton-X100 in PBS for 30 minutes at room temperature (RT). Cells were rinsed with PBS and incubated in blocking solution (1% BSA in PBS) for 30 minutes at RT. Primary antibody (Anti-MHC my32, Sigma-Aldrich) at a concentration of 0.5 µg/ml was added in blocking solution for 2 hours at RT. Cells were rinsed

with PBS and the secondary antibody labeled with Alexa Fluor 555 (Life Technologies) at a final concentration of 20 µg/µl was added in blocking solution for 2 hours, in the dark, at RT. Lab-Tek chambers were rinsed with PBS and slides were mounted with VectaShield mounting medium (Vector laboratories) containing DAPI.

Sarcomeric organization (resulting from MHC labeling) was visualized by confocal microscopy (LSM 780, Cark Zeiss MicroImaging GmbH). Fluorophore excitations were performed simultaneously using 405 nm diode for DAPI imaging and 514 nm laser line for Alexa Fluor 555. Images were acquired with a Plan Apochromat 40X / 1.3 numerical aperture oil immersion objective, using Zen software (Carl Zeiss MicroImaging GmBH). Seven images from two different Lab-Tek chambers were acquired per condition. Four morphometric parameters were determined: the M-line, the dark band and I-band widths and the sarcomere length (µm). For each parameter, 1 myotube per image was selected, and ten measurements were carried out per myotubes; in total 70 measurements were determined per parameter. Measurements were realized with ImageJ software.

Protein extractions

Whole cellular extract **-** C2C12 myotubes were rinsed three-times in cold PBS. They were then scrapped in cold RIPA lysis buffer (10 mM Tris/HCl, pH 7.4; 150 mM NaCl; 1 mM EDTA; 1 % Triton X-100; 0.5% sodium deoxycholate; 0.1 % SDS) containing anti-proteases (Complete EDTA-free, Roche Diagnostic), anti-phosphatases (Phos-Stop, Roche Diagnostic), and 50 µM PUGNAc (O-(2-acetamido-2-deoxy-D-glucopyrano-silidene) amino-N-phenyl-carbamate, Sigma-Aldrich). Proteins extracts were sonicated using Ultra-sonic Cell Disruptor, and then homogenized with gentle agitations for 1 hour at 4°C. Protein concentration of these whole cellular extracts was done using Bradford assay (Biorad).

Protein subfractionation **-** Myotubes proteins were subfractionated as previously described [45]. Briefly, myotubes were scrapped in cold lysis buffer (50 mM Tris/HCl, pH 7.5; 5 mM EGTA; 2 mM EDTA; 5 mM DTT; 0.05 % digitonin) containing inhibitors as described just above. Cell lysates were rapidly sonicated and then centrifuged at 9500 rpm for 30 minutes at 4°C. Supernatants (corresponding to the cytosol-enriched fraction) were discarded. The resulting pellets were solubilized in cold lysis buffer containing 1 % Triton X-100, homogenized and centrifuged at 9500 rpm for 30 minutes at 4°C. Supernatants (corresponding to the membrane-enriched fraction) were removed and remaining pellets (corresponding to the myofilament-

enriched fraction) were solubilized in cold RIPA lysis buffer. The protein content of the myofilament-enriched fraction was assayed using the Bradford's method.

Native extract **-** C2C12 myotubes were rinsed three-times in cold PBS. They were then scrapped in cold native buffer (20 mM Bis-Tris, pH 7.0; 500 mM 6-amino-n-caproic acid; 20 mM NaCl; 2 mM EDTA; 10% glycerol) containing inhibitors. Native-proteins extracts were gently and rapidly sonicated, and then homogenized with gentle agitation for 1 hour at 4°C. Protein estimation was done using Bradford assay.

OGA activity assay **–** O-GlcNAcase was assayed as reported by Zachara and colleagues [43] using 50 µg of whole extracts (extraction with RIPA buffer without PUGNAc) were incubated in 96 well-plates in OGA buffer (50 mM sodium cacodylate, pH 6.4; 5 mM N-acetylgalactosamine (GalNAc), anti-phosphatases and anti-proteases); 50 mM NA_2CO_3; 10 mM *p*-nitrophenol N-acetylglucosaminide (*p*NP-GlcNAc, Sigma-Aldrich)) in a final volume of 100 µl. A blank reaction without whole extract was included to remove the background. Plates were then incubated 2 hours at 37°C. The reaction was stopped by the addition of 100 µl of 500 mM Na_2CO_3 were added to each well to stop the reaction. Absorbance was read at 400 nm on a micro-plate reader. OGA activity was calculated according to the following equation: mM of *p*NP-GlcNAc released = A_{400}/(17.4 x 10 mM^{-1} . cm^{-1} x pathlength).. The molar extinction coefficient for *p*NP-GlcNAc is 17.4 x 10 $mM^{-1}.cm^{-1}$ at pH 10. The pathlength for 200 µl on a 96-well plate is 0.71 cm.

Immunoprecipitation experiments **–** Immunoprecipitation was performed on 100 µg of proteins extracted in RipA buffer. Samples were pre-cleared with protein G coupled on magnetic beads (Millipore). Non-retained samples were incubated with the RL-2 antibody (MA1-072, Thermo Scientific, at a final concentration of 20 µg/ml) overnight at 4°C with gentle agitation, followed by 2 hours incubation at 4°C with magnetic beads (1:5; v/v). Beads were washed sequentially using RipA; RipA + 0.5 NaCl; RipA/TNE (TNE: 10 mM Tris/HCl, pH 7.4; 150 mM NaCl; 1 mM EDTA) (50:50, *v/v*), and the last one with TNE. Beads were finally resuspended in Laemmli buffer (62.5 mM Tris/HCl, pH 6.8; 10% glycerol; 2% SDS; 5% ß-mercaptoethanol; 0.02% bromophenol blue) and boiled for 10 min. The remaining soluble fractions, corresponding to immunoprecipitated proteins were analyzed using SDS-PAGE and western blot as described below.

Co-immunoprecipitation experiments **–** Co-immunoprecipitation was performed on 100 µg of proteins extracted in native buffer. Samples were pre-cleared with protein G coupled on magnetic beads. Non-retained samples were incubated with primary antibody (at a final concentration of 10 µg/ml) overnight at 4°C with gentle agitation, followed by 2 hours incubation at 4°C with magnetic beads (1:5; v/v). Beads were washed five times using the native buffer with strong agitations. Beads were finally resuspended in Laemmli buffer and boiled for 10 min. The remaining soluble fractions, corresponding to co-immunoprecipitated proteins were analyzed using SDS-PAGE and western blot as described below.

SDS-PAGE and western blot analysis **–** Co- and immunoprecipitated samples, whole extracts and myofilament-enriched fractions (previously boiled in Laemmli buffer) were resolved by SDS-PAGE. Proteins were separated on Mini-PROTEAN TGX Stain-Free (SF) 7.5% precast polyacrylamide gels (Biorad); an internal standard was loaded on each gel. Stain-Free technology contains a proprietary trihalo compounds which react with proteins, rendering them detectable with UV exposures. SF imaging was performed using ChemiDoc MP Imager and Image Lab 4.0.1 software (Biorad) with a 5-min stain activation time, and total protein images were therefore obtained. Proteins were then transferred to 0.2 µm nitrocellulose sheet using the Trans-Blot Turbo Transfer System (Biorad). The quality of transfer was controlled by imaging membranes using the SF technology. The membranes were then washed in TBST (15 mM Tris/HCl, pH 7.6; 140 mM NaCl; 0.05 % Tween-20) and blocked in 5 % non-fat dry milk or BSA in TBST. Membranes were then blotted with primary antibodies (α-actinin, ab9465, Abcam; αB-crystallin, ab13497, Abcam; desmin, ab6322, Abcam; filamin-C, HPA006135, Sigma-Aldrich; MHC, my32, Sigma-Aldrich; moesin, ab52490, Abcam; RL-2, MA1-072, Thermo Scientific) in blocking solution overnight at 4°C or 2 hours at room temperature. After 3x10 minutes washes in TBST, membranes were probed with secondary antibodies (IgG, HRP linked, 7076 or 7074S, Cell signaling) in blocking solution for 2 hours at RT, and finally extensively washed in TBST. All experimental procedures, such as the blocking solutions as well as the dilutions of primary and secondary antibodies were optimized for each antibody. Chemiluminescence detection was carried out using ECL Clarity (Biorad), and images capture were done with ChemiDoc MP. All the images were analyzed using the Image Lab 4.0.1 software. Normalization of protein signal intensities was carried out following the quantification of respective total protein level on SF images and internal standards.

Red Native-PAGE (RN-PAGE): western blot and colloidal blue-stain - RN-PAGE was performed according to previously Native-PAGE protocols with minor changes [46] [47] on Biorad Protein II XL Cell. Native extracts were separated on 5% acrylamide resolving gel. The stacking gel was composed of 4% acrylamide/bisacrylamide (37.5:1), 0.125 M Tris/HCl pH 6.8, 0.034% APS, 0.06% TEMED, 0.012% Red ponceau S, and the separating gel of 5% acrylamide/ bisacrylamide (37,5:1), 0.375 M Tris/HCl, pH 8.8, 0.034% APS, 0.06% TEMED, 0.012% Red ponceau S. Electrophoresis was performed at 150 V in the stacking gel and at 100 V in the separation gel at 4°C for a total duration of 27 hours. The run was performed with the cathode buffer (15 mM Bis-Tris, pH 7.0; 50 mM Tricine; 0.012% Red Ponceau S) and the anode buffer (50 mM Bis-Tris, pH 7.0).

Following RN-PAGE, proteins were transferred to 0.2 µm nitrocellulose sheet (Hybond, GE Healthcare) in transfer buffer (20 mM Tris base; 150 mM glycine; 20% methanol; 0.025% SDS). Quality of transfer was verified by Ponceau staining. Antibody incubations and detection of protein signals were carried out as described above. Quantification of protein level was done using the Image Lab 4.0.1 software.

In other cases, gels were colloidal blue-stained. Briefly, gels were fixed in 50% ethanol and 2% phosphoric acid overnight at RT, and then washed 2x45 minutes in 2% phosphoric acid. They were incubated in a solution of 15% ammonium sulfate, 2% phosphoric acid, 17% ethanol for 20 minutes, and finally in the same buffer containing 0.1% Coomassie Brillant Blue G-250 (Sigma-Aldrich). After 3 days of staining, gels were washed in water, image captures were done with ChemiDoc MP and gel bands were analyzed using Image Lab 4.0.1 software.

"In-gel" digestion of proteins - Differential bands were excised from native gels. Gel bands were destained in 0.1 M ammonium bicarbonate (NH_4HCO_3) for 15 minutes, and an equal volume of acetonitrile (ACN) was added for 20 minutes. These steps were repeated until bands were completely destained, and gels pieces were then dehydrated and shrunk in a vacuum centrifuge. Proteins were reduced at 56°C for 30 minutes with 10 mM dithiothreitol in 0.1 M NH_4HCO_3 and submitted to alkylation in 55 mM iodoacetamide in 0.1 M NH_4HCO_3 for 30 minutes in the dark. Gel pieces were washed with 0.1 M NH_4HCO_3 for 15 minutes, and then dehydrated and dried as described previously.

For "in-gel" digestion, gel pieces were rehydrated in the digestion buffer containing 0.1 M NH_4HCO_3, 5 mM $CaCl_2$, and 12.5 ng/µl trypsin, for 15 minutes at 4°C. The excess of buffer was

removed, and the gel pieces were covered with the digestion buffer without trypsin. Digestion was performed overnight at 37°C.

After "in gel" trypsic digestion, peptides were extracted by the addition of 50 µl of 25 mM NH_4HCO_3, gel pieces were shaken for 15 minutes, and the supernatant was collected. Two successive extractions were performed with 45% ACN/0.1% TFA for 15 minutes. The last extraction was realized with 95% ACN/0.1% TFA for 15 minutes. Extracts were pooled, dried in a vacuum centrifuge, and stored at -20°C.

Nano-LC - Following trypsin digestion, the peptides were separated on an U3000 nano-LC system (Dionex-LC-Packings, Sunnyvale, CA, USA). After a standard pre-concentration step (C18 cartridge, 300 µm, 1 mm), the peptide samples were separated on an Acclaim PepMap100, C18 column (75 µm i.d. x 15 cm, 3 µm, 100 Å) using an ACN gradient (no ACN over 3 minutes, followed by gradient from 0% to 15% over 7 minutes, 15% to 65% over 42 minutes, 65% to 90% over 5 minutes and, lastly, 6 minutes in 90% of ACN). The flow was set to 300 nl/min and a total of 110 fractions were automatically collected (one every 30 s) on an AnchorChip™ 600 MALDI target by using a Proteineer^{TM} fraction collector (Bruker Daltonics). Matrix (2 µl of 0.3 mg/ml in acetone: ethanol: 0.1% TFA-acidified water, 3:6:1 v/v/v) was added to each deposit during the collection process.

MALDI-TOF/TOF - The MS (reflectron mode) and MS/MS (lift mode) measurements were performed off-line in automatic mode on an Ultraflex™ II TOF/TOF mass spectrometer (Bruker Daltonics) running FlexControl™ 3.3 software (Bruker Daltonics). External calibration over the 1,000-3,500 mass range was performed using the $[M+H]^+$ mono-isotopic ions from bradykinin 1-7, angiotensin I, angiotensin II, substance P, bombesin and adrenocorticotropic hormone (clips 1–17 and clips 18–39) from a peptide calibration standard kit (Bruker Daltonics). Briefly, each MS spectrum was acquired by accumulating data from 500 laser shots with a 25 kV accelerating voltage, a 26.3 kV reflector voltage and a 160 ns pulsed ion extraction. Peptide fragmentation was driven by Warp-LC software 1.2 (Bruker Daltonics), according to the following parameters: signal-to-noise ratio >15, more than 3 MS/MS per spot if the MS signal was available, 0.15 Da of MS tolerance for peak merge and the elimination of peaks that appeared in over 35% of the fractions. Precursor ions were accelerated to 8 kV and selected in a timed ion gate. Metastable ions generated by laser-induced decomposition were further accelerated by 19 kV in the lift cell and their masses were measured in reflectron mode. For precursor and daughter ions, each MS/MS spectrum was produced by accumulating data from 200 and 1,000 laser shots,

respectively. Peak lists were generated from MS and MS/MS spectra using Flexanalysis™ 3.3 software (Bruker Daltonics). Proteins were identified on the basis of peptide fragmentation fingerprints, according to published guidelines. Database searches with Mascot 2.3.02 (Matrix Science Ltd, London, UK) were performed in the UnitProt database via ProteinScape 2.1 (Bruker Daltonics). Taxonomy was restricted to Rodentia; a mass tolerance of 75 ppm and 1 missing cleavage site for PMF and an MS/MS tolerance of 0.5 Da and 1 missing cleavage site for MS/MS searching were allowed. Carbamidomethylation of cysteine and oxidation of methionine residues were considered as fixed and variable modifications, respectively. The relevance of protein identities was judged according to the probability-based Molecular Weight Search score MOWSE (calculated with $p< 0.05$).

Statistical analysis **-** All treatments were performed in biological triplicates from 3 independent cultures. All quantitative results were presented as means ± SEM. Significance of intergroup differences was examined using Mann-Whitney tests and t-tests (GraphPad Prism software). Differences were considered statistically significant when $p<0.05$.

RESULTS

Modulation of the global level of O-GlcNAcylation in C2C12 myotubes: O-GlcNAc level variations are more sensitive and dynamic on myofilament proteins than whole extract - To determine the effects of O-GlcNAcylation variations on the sarcomeric structure in mature C2C12 myotubes, described as a suitable skeletal muscle model for this study [48], we modulated the global O-GlcNAcylation level using a pharmacological molecule. Thus, to increase the O-GlcNAc level, Thiamet-G, an OGA inhibitor, was used [44].

For the increase of O-GlcNAc level, three concentrations of Thiamet-G were chosen (0.1, 0.5 and 1.0 µM) for 4 hours. For each treatment, the myotube and sarcomere maturations determined using fusion index and western blot of myosin chain respectively, as well as the cell viability, by using MTT assay, were not altered (data not shown).

To quantify the global O-GlcNAc level variations, western blots were performed using RL2-antibody on whole protein extract and on myofilament-enriched fraction. The whole protein pattern (Stain-free) and the RL-2 profiles were presented on the top of figure 1, while the quantification of the variation of O-GlcNAc level were presented above. As shown on whole extract (Fig. 1A), Thiamet-G led to a significant increase of O-GlcNAc level (1.33±0.10 a.u., $p<0.05$ and 1.50±0.08 a.u., $p<0.001$, for 0.1 µM and 0.5 µM of Thiamet-G, respectively); we also observed that the increase of O-GlcNAc pattern with 0.5 µM or 1.0 µM of Thiamet-G were similar. The inhibitory effect of Thiamet-G was not reversible on whole protein extract, at least for 4 hours post-treatment (no significant difference: NSD between 0.5 µM of Thiamet-G and 4 hours of post-treatment without 0.5 µM of Thiamet-G). On the myofilament-enriched fraction (Fig. 1B), we measured a significant and dose-dependent increase of O-GlcNAc level with Thiamet-G treatments (1.52±0.04, 1.74±0.09 and 2.07±0.14 a.u., for 0.1, 0.5 and 1 µM of Thiamet-G, respectively, $p<0.001$) (Fig. 1B). The O-GlcNAc level returned gradually to control value during the reversion protocol after two hours (1.56±0.09 a.u., $p<0.01$ compared to control), and four hours (1.25±0.08 a.u., NSD compared to control) when Thiamet-G was removed from culture medium. In particular, a significant difference ($p<0.05$) between treatment with 0.5 µM of Thiamet-G and 4 hours post-treatment without 0.5 µM of Thiamet-G was observed. So, as shown in Fig. 1B, the modulation of O-GlcNAc levels was more sensitive and dynamic on the myofilament-enriched fraction than total proteome in C2C12 myotubes. Similar results were obtained using western blot WGA-HRP to detect O-GlcNAc modified proteins (data not shown).

To demonstrate the inhibition of OGA by Thiamet-G, we measured the OGA activity in each experimental condition (figure 1, supplemental data). A dose-dependent decrease of the OGA activity was observed with Thiamet-G (supp. Fig. 1A), from 0.074±0.005 nmol.µg^{-1} proteins.min^{-1} in untreated myotubes, to 0.065±0.005, 0.051±0.005 ($p<0.01$) and 0.040±0.004 nmol.µg^{-1} proteins.min^{-1} ($p<0.001$) for Thiamet-G concentrations of 0.1, 0.5 and 1 µM respectively. The OGA expression was not altered (data not shown). Moreover, after two ($p<0.05$) and four hours (NSD) without 0.5 µM of Thiamet-G, OGA activity tended to return gradually to control value (supp. Fig. 1B). The OGA expression was not altered (data not shown). To sum up, Thiamet-G allowed a reversible decrease of the OGA activity in C2C12 myotubes.

Changes in sarcomeric morphometry through the variation of O-GlcNAc level on myofilament-enriched fraction **-** In order to measure the impact of the O-GlcNAc level variations on the sarcomeric structure, we investigated, using confocal microscopy, the sarcomeric morphometry after the immunofluorescent labeling of Myosin Heavy Chain (Fig. 2A). Four essential parameters characterizing the sarcomeric morphometry were measured: the dark band, I-band and M-line widths and, *in fine*, the sarcomere length (Fig. 2B). The different distances variations were presented, according to the O-GlcNAc level variations on myofilament-enriched fraction determined above (Fig. 2C). The corresponding values were presented in supplemental data as table 1. The average length for sarcomere for untreated myotubes was 2.74 µm, while the width for dark band, M-line, and I-band were 0.58 µm, 0.23 µm and 1.21 µm, respectively (dotted line in Fig. 2C).

Interestingly, linear variations between increased dark band, M-line widths as well as decreased I-band width and sarcomere length and O-GlcNAcylation level were measured (Fig. 2C and supp. table 1). Indeed, a 50% increase of the global O-GlcNAc level led to the increase of the dark-band and M-line widths (0.60±0.01 µm, $p<0.05$ and 0.26±0.01 µm, $p<0.001$ respectively), while the I-band width and the sarcomere length decreased at 1.01±0.01 µm, $p<0.001$ and 2.59±0.02 µm, $p<0.001$, respectively. The increase of the dark-band and M-line widths reached 0.62±0.01 µm, $p<0.001$ and 0.29±0.01 µm, $p<0.001$, respectively, while the decrease of the I-band width and the sarcomere length reached 0.88±0.01 µm, $p<0.001$ and 2.52±0.01 µm, $p<0.001$ for 75% increase of the global O-GlcNAc level. Finally, a two-fold increase of the global O-GlcNAc level led to the increase of the dark-band and M-line widths to 0.62±0.01 µm, $p<0.001$ and 0.30±0.01 µm, $p<0.001$, respectively, while the I-band width

(0.80±0.01 µm, $p<0.001$) and the sarcomere length (2.49±0.02 µm, $p<0.01$) decreased. Interestingly, the sarcomeric morphometry (whatever the width or length considered) tended to return to control values after 4 hours without 0.5 µM of Thiamet-G, or after 24 hours without 25 µM of DON (supp. table 1). As can be seen on the curves (Fig. 2C), these increased and decreased distances varied linearly to the myofilament O-GlcNAc level.

We schemed on Fig. 2D the variations of sarcomeric morphometry according to the global O-GlcNAcylation variations; as shown on the schematic sarcomere, the sarcomeric structure was modulated proportionally to the O-GlcNAc level variations of the myofilament-enriched fraction.

Protein complexes, including structural proteins, were modulated through O-GlcNAc variations - In view of the morphometric changes of sarcomere according to the O-GlcNAc level, we determined if some protein complexes within sarcomere structure were modulated, and so which could be potentially involved in the sarcomeric structure changes.

Red-Native PAGE was performed to detect protein complexes. This original method used Ponceau-S to help the electrophoretic separation of proteins complexes, in their native form, according to their molecular weight (as described Dráb and colleagues [47]). Without denaturing agents, it allowed separating proteins in native form to maintain protein complexes through the maintenance of protein-protein interactions. After colloidal blue-staining, native protein bands were visualized in gel, corresponding to different protein complexes. Native protein profiles from whole extracts visualized on the Red-Native gel were presented in figure 3. As illustrated in the expanded regions of the presented gel in figure 3, six regions presented dose-dependent pattern variations corresponding to changes in their electrophoretic mobility. In particular, within regions 2 to 6, electrophoretic mobility seemed to be reduced when the O-GlcNAcylation level increased (Thiamet-G treatments of myotubes).

These bands of interest were cut from the gel and submitted to trypsin digestion in order to identify the constitutive proteins of these complexes (complete list of identified protein is given in supplemented table 2). A large number of proteins have been identified within each area, suggesting that several protein complexes might co-migrate within the same bands in this one-dimensional gel electrophoresis. Interestingly, the identified proteins belong to different families of proteins, corresponding so to a wide range of functions. Indeed, majority of identifications was structural proteins, heat-shock proteins, glycolytic proteins, and proteins related to degradation

systems. Among them, some proteins could be more particularly candidates to explain sarcomeric structure changes, in particular: filamin-C, desmin, αB-crystallin, moesin and α-actinin (table 1). These results have clearly shown that some key proteins of the sarcomeric structure have been identified within protein complexes finely modulated by O-GlcNAc level variations.

Protein-protein interactions: focus on candidate proteins in complexes - The results described just above suggested that some protein-protein interactions, involving key structural proteins, were modulated consecutively to the global O-GlcNAcylation variations on C2C12 myotubes. To define the involvement of theses structural proteins in the remodeling of sarcomere, we analyzed the remained proteins complexes after co-immunoprecipitation of these protein candidates. As indicated by full arrows in Fig. 4B-F, when structural proteins were co-immunoprecipitated with their proteins partners, we observed on Red-native PAGE the disappearance of the bands 1 to 3 (as shown in Fig.3) which were modulated consecutively to the global O-GlcNAcylation variations. These data supported the involvement of filamin-C, moesin, αB-crytallin, desmin and α-actinin in the complexes modulated consecutively of a global O-GlcNAcylation variation.

Interestingly, some of these proteins presented a modulation of their O-GlcNAc level following the Thiamet-G treatments of C2C12 myotubes. Indeed, we determined the O-GlcNAcylation variation on filamin-C, desmin and αB-crystallin, by using RL-2 immunoprecipitation. Results were presented on figure 5. For the first time, filamin-C was shown to be O-GlcNAcylated, but it did not present any change in its O-GlcNAc level following Thiamet-G treatments despite a decrease tendency ($p=0.08$, Fig. 5A). Moreover, we have also quantified any change in the O-GlcNAcylation level of αB-crystallin in Thiamet-G-treated myotubes compared with control (Fig. 5B). In contrast, as shown on Fig. 5C, the O-GlcNAc level decreased on desmin in Thiamet-G-treated myotubes (0.71 ± 0.09, $p<0.05$). Lastly, while moesin was described to be O-GlcNAcylated in pancreatic β-cell [49], such as α-actinin in soleus [35], we did not detect these proteins in these experiments.

According to the western blot experiments following Red-Native PAGE presented on figure 6, native-desmin profile possessed three predominant bands (Fig. 6A). The intensity of the third band changed with O-GlcNAcylation level, and increased ($p<0.05$) in Thiamet-G treated cells; it is worth to note that the total expression of desmin was not modified consecutively to

pharmacological treatments (Fig. 6F). We also observed that several bands were detected in the native profile of αB-crystallin. In opposite to desmin, the intensity of the αB-crystallin signal in the third band decreased with Thiamet-G ($p<0.01$, Fig. 6B), while the global expression of αB-crystallin was not modified as measured in western blot performed after SDS-PAGE (Fig. 6G). Interestingly, both described native-bands were almost completely superposed.

We also analyzed the expression of α-actinin, moesin and filamin-C. The α-actinin and moesin signals seemed to be changed in some characteristic native bands (Fig. 6C and 6D). Their signal intensities decreased in Thiamet-G treated cells. Following SDS-PAGE, α-actinin was not changed (Fig. 6H). However, moesin expression was modulated (Fig. 6I). Indeed, moesin expression decreased with Thiamet-G ($p<0.05$) and could partially explain the decrease the signal measured in native conditions (Fig. 6D). Subsequently to RN-PAGE (Fig. 6E) and SDS-PAGE (Fig. 6J), there were no changes in filamin-C expressions.

Thus, in particular for desmin and αB-crystallin, the distribution of these proteins in some native bands seemed to be modulated following Thiamet-G treatments, without changes of its total expression, and could mean a modulation of protein-protein interactions.

Finally, we focused on protein-protein interactions between desmin and αB-crystallin; indeed, modulated native-bands were almost completely superposed (Fig. 6A and 6B). Interactions between desmin and the heat shock protein αB-crystallin have been described to play a crucial role on desmin aggregation and localization [50]. Co-immunoprecipitations (Co-IP) of αB-crystallin (Fig. 7A), and desmin (Fig. 7B), followed by western blot (WB) were performed. Co-IP of αB-crystallin, followed by its proper detection on western blot, showed that the expression of αB-crystallin did not change after C2C12 myotubes treatment, which is in agreement with data presented just above (Fig. 6G). Similar data were obtained for desmin, as expected (Fig. 6F). Co-IP αB-crystallin/WB desmin experiments (Fig. 7A) showed that interactions between αB-crystallin and desmin increased (1.40±0.16 a.u., $p<0.05$) when C2C12 myotubes were treated with Thiamet-G. The reciprocal experiment (*i.e* Co-IP desmin/WB αB-crystallin, Fig. 7B) showed similar variations. Indeed, the desmin/αB-crystallin interaction increased with Thiamet-G (1.35±0.24 a.u., $p=0.07$).

Taken together, these results showed that some protein-protein interactions could be modulated consecutively to global O-GlcNAcylation variation, especially the interaction between

desmin and αB-crystallin. Importantly, these proteins are involved in the maintenance of the sarcomeric organization.

DISCUSSION

Within the skeletal muscle sarcomere, many myofibrillar proteins are O-GlcNAc-modified, which could be related to the localization of OGT and OGA, the enzymes responsible for O-GlcNAc addition and removal respectively, at the Z-line [33]. Among the modified proteins, several contractile and regulatory proteins were identified and could be related to the modulation of skeletal muscle contractile activity by the O-GlcNAcylation [32] [34] [35]. However, several key structural proteins of the sarcomere were also identified to be O-GlcNAcylated, and the role of this PTM in the regulation of the sarcomeric organization, crucial for muscle physiology, should be considered. Thus, to clarify this issue, the purpose of our study was to investigate the effect of a modulation of the global O-GlcNAcylation level on the sarcomere structure in C2C12 myotubes.

The most important finding of this paper was the modulation of the sarcomere structure through the O-GlcNAcylation level variations. Immunofluorescence labeling of MHC enabled to measure morphometric parameters of the sarcomere to study its structure. Linearly to the global O-GlcNAc level, we showed that the M-line and the dark-band widths increased. On the contrary, the I-band width and the sarcomere length decreased. In this way, we have clearly demonstrated that sarcomere organization was dynamically modulated. Previously, some studies had already described alterations in the sarcomeric morphometry such as in desmin- [51] and nebulin-mutant mice [52] [53], or in mice deficient in titin's I-band/A-band junction [54]. In a same way, some alterations of the sarcomeric organization have been described in the atrophied soleus following a long-term hindlimb unloading model in the rat [55].

To better understand the role of O-GlcNAcylation in the sarcomere organization, we modulated the global O-GlcNAcylation level in C2C12 myotubes. Interestingly, we showed that the variation of the global O-GlcNAc level was more sensitive and dynamic in the myofilament-enriched fraction than in whole cellular extract. This could be explained by the localization of OGT and OGA at the Z-line [33]. Indeed, previous data reported that O-GlcNAcylation, through OGT and OGA, was regulated in response to several stimuli, and in a dynamic manner [56].

Nowadays, the Z-line is not considered as a passive constituent of the sarcomere, but on the contrary as a nodal point [7]. This key interface was described as an anchoring and exchange zone of various cytoskeletal, signaling and apoptotic proteins, and as well as enzymes such as glycolytic proteins organized in metabolon [57]. Interestingly, these proteins have been identified within modulated protein complexes belonging to the Z-line. Therefore, by the varied nature of its composition, the Z-line was often sensitive to a multitude of intra- and extracellular stimuli, and was constantly remodeled [58]. In this way, the sarcomere could be quickly and locally modulated. Taken together, these evidences could explain a fine modulation of the O-GlcNAcylation on the sarcomere, which could lead to a fine modulation of the sarcomere remodeling.

Previous studies showed that an increase of the global O-GlcNAcylation level was a hallmark of the diabetic heart associated to an alteration of the calcium sensitivity. Indeed, in STZ-diabetic cardiac muscle, OGA and OGT were delocalized, their activities were altered, and the interactions between OGA, α-actin, tropomyosin, and myosin light chain 1 were increased, leading to an increase of their O-GlcNAcylation state. The use of a bacterial analogue of OGA – CpOGA – led to a decrease of O-GlcNAcylation on these specific myofilament proteins and to the restoration of the calcium sensitivity [59]. By the way, in our study, increase of the global O-GlcNAcylation level induced by Thiamet-G could lead to a modulation of protein-protein interactions resulting to a potent physiological consequence on the sarcomeric organization.Using Red-Native PAGE, we demonstrated that some protein complexes were modulated consecutively to the variation of the global O-GlcNAc level. A multitude of proteins have been identified in these protein complexes including myofibrillar proteins. Among them, there were some structural proteins, key regulators of the sarcomere structure that have been identified previously to be O-GlcNAc-modified. Moreover and except for moesin, the expression of these proteins didn't change following treatments, but the O-GlcNAc level varied on some proteins, in particular desmin. Interestingly, desmin presented a decrease of its O-GlcNAcylation level in Thiamet-G treated myotubes. We also observed variations in the amount of these proteins in some of the proteins complexes. Thus, we concluded that protein-protein interactions changed, reflected by the modulation of these protein complexes observed in native-PAGE, which strongly supported that O-GlcNAcylation modulated the structural interactome. A simplified scheme of the interactome of the present identified "candidate" proteins, that could explain the modulation of the sarcomeric structure following O-GlcNAc variations, was presented figure 8.

One of the identified proteins in complexes was α-actinin. Based on our western blot from RN-PAGE, some α-actinin interactions seemed to be altered. This protein is fundamental for sarcomere organization because it is the major component of the nodal Z-line [60]. By the way, α-actinin was described as the major multivalent platform for a number of protein-protein interactions with cytoskeletal and regulatory proteins. Indeed, it bound sarcomeric actin to stabilize the contractile apparatus and connected it to diverse signaling pathways [61]. Interestingly, moesin operated in both mechanisms. Indeed, this cytoskeleton protein changed it conformation to associate the sarcomere to the sarcolemma. For example, after phosphorylation on threonine 558, the conformation of moesin changed, leading to its binding to F-actin to activate other binding partners [62]. Moreover, abnormal moesin, localized mainly to the membrane, increased actin polymerization leading to cardiopathy, and altered RhoA/ROCK pathway leading to diabetes complications [63].

We also identified desmin as component of modulated protein complexes. Mainly located around the Z-line and at the M-line, this intermediate filament protein is essential for the structural integrity of the sarcomere [64]. Desmin anchored myofibril to the sarcolemma and other structural elements of the cell, but also integrated many protein complexes within the contractile apparatus and finely maintained its organization [65]. Moreover, desmin structure was highly dynamic [66]. In this present study, we showed that desmin was modulated in some protein complexes according to the global level of O-GlcNAcylation. This data could be supported by two hypotheses. Firstly, several recent studies described desmin as a substrate of a wide spectrum of post-translational modifications (for review [67] [68]). Its degree of polymerization was dependent on its state of phosphorylation [11] [40], but could also depend on its level of O-GlcNAcylation since it was demonstrated that polymerization of cytokeratins 8 and 18 [69] or tubulin [70] was modified through O-GlcNAcylation. Secondly, desmin integrity was also regulated by numerous heat shock proteins. Phosphorylation of HSP25 at ser15 seemed to change the localization of desmin at the Z-line and its colocalization with alpha-actinin. Interestingly, this relocalization was correlated with the formation of disorganized Z-lines [71]. Then, interactions between αB-crystallin, another heat shock protein, and desmin filaments played a crucial role on its aggregation and localization [50]. To date, there are no available data on O-GlcNAcylation affecting such interactions although desmin possessed lectin domains [42] and its interactome was highly complex [72]. However, some works showed O-GlcNAcylation [73] of αB-crystallin played a crucial role on its translocation and stabilization to cytoskeletal elements. Interestingly, from our native western blot as well as co-IP/WB experiments, we

showed herein that interactions between desmin and αB-crystallin were modulated consecutively to global O-GlcNAcylation changes in C2C12 myotubes. However, the effects of αB-crystallin toward desmin filaments depending on the O-GlcNAcylation remained to be elucidated. Indeed, changes to any interacting region of αB-crystallin can produce positive as well as negative effects on desmin [74]. According to the interaction domain of the αB-crystallin, its binding with desmin, the self-assembly and the filament-filament interactions of the desmin were incredibly modified [74], and could explain more precisely some effects on the sarcomere structure.

To conclude, our study focused on a modulation of the global O-GlcNAcylation level in particular on myofilament proteins in C2C12 myotubes. These variations affected the sarcomere structure and some protein complexes including structural proteins that regulated the sarcomere organization. Finally, some interactions of these proteins seemed to be altered and emphasized the role of O-GlcNAcylation in the dynamic sarcomere remodeling. Interestingly, key structural proteins such as desmin, αB-crystallin, and filamin-C, belong to structural complexes modulated by O-GlcNAcylation, their location within protein complexes being themselves modified. Importantly, these proteins are affected by mutations which are directly involved in myofibrillar myopathies [75], characterized by a dramatic sarcomere disorganization. In the same way, α-actinin mutations are often associated with myopathies, showing the importance of the nodal Z-line [76]. Finally, moesin modifications could associate muscular diseases and diabetes complications [63].

Altogether, this paper clearly argues in favor of the key role of O-GlcNAcylation in the sarcomeric organization in skeletal muscle, such as protein localization within protein complexes, and/or protein-protein interactions through the O-GlcNAc level variations. Previously, O-GlcNAcylation was described as a regulator of myocardial contractile function [77] and as a modulator of contractile activity in striated muscle [37]. Number of studies (for review [32]) had identified some O-GlcNAcylation sites in contractile/regulatory myofilament proteins leading to new insights in the understanding of the calcium sensitivity/affinity alterations following O-GlcNAc variations in sarcomere. In order to better understand O-GlcNAcylation as a key modulator of the sarcomeric organization, future investigations must identify O-GlcNAc sites in structural myofilament proteins. Finally, it would be essential in the future to consider O-GlcNAcylation as an important actor of sarcomeric remodeling resulting from several disorders such as diabetes, myopathies and cardiomyopathies.

ACKNOWLEDGMENTS

We thank Johan Hachani (Plateforme de spectrométrie de masse et d'analyse de l'Artois) for his help with the mass spectrometry analysis.

This work was supported by grant from the Région Nord-Pas-de-Calais 2011 (Emergent Research Project, n°12003803) and the Centre National d'Etudes Spatiales (N° 4800000784). Matthias Lambert is a recipient from the French Ministry for Research and Tertiary Education.

CONFLIC OF INTEREST

The authors declare that they have no conflict of interest.

AUTHOR CONTRIBUTIONS

Matthias Lambert: Performed the experiments, analyzed the data and wrote the paper; Elodie Richard, Sophie Duban-Deweer, Frederic Krzewinski: contributed to acquisition and analysis of the data; Barbara Deracinois and Erwan Dupont: Performed the experiments; Bruno Bastide: conceived the experiments, and wrote the paper; Caroline Cieniewski-Bernard: conceived and designed the experiments, performed the experiments, analyzed the data, and wrote the paper.

REFERENCES

[1] M. Gautel, The sarcomeric cytoskeleton: Who picks up the strain?, Curr. Opin. Cell Biol. 23 (2011) 39–46. doi:10.1016/j.ceb.2010.12.001.

[2] J.W. Sanger, J. Wang, Y. Fan, J. White, J.M. Sanger, Assembly and dynamics of myofibrils, J. Biomed. Biotechnol. 2010 (2010). doi:10.1155/2010/858606.

[3] O. Boonyarom, K. Inui, Atrophy and hypertrophy of skeletal muscles: Structural and functional aspects, Acta Physiol. 188 (2006) 77–89. doi:10.1111/j.1748-1716.2006.01613.x.

[4] K. a Clark, A.S. McElhinny, M.C. Beckerle, C.C. Gregorio, Striated muscle cytoarchitecture: an intricate web of form and function., Annu. Rev. Cell Dev. Biol. 18 (2002) 637–706. doi:10.1146/annurev.cellbio.18.012502.105840.

[5] Y. Au, The muscle ultrastructure: a structural perspective of the sarcomere., Cell. Mol. Life Sci. 61 (2004) 3016–33. doi:10.1007/s00018-004-4282-x.

[6] S. Lange, E. Ehler, M. Gautel, From A to Z and back? Multicompartment proteins in the sarcomere., Trends Cell Biol. 16 (2006) 11–8. doi:10.1016/j.tcb.2005.11.007.

[7] D. Frank, C. Kuhn, H. a. Katus, N. Frey, The sarcomeric Z-disc: A nodal point in signalling and disease, J. Mol. Med. 84 (2006) 446–468. doi:10.1007/s00109-005-0033-1.

[8] W.M. Obermann, M. Gautel, K. Weber, D.O. Fürst, Molecular structure of the sarcomeric M band: mapping of titin and myosin binding domains in myomesin and the identification of a potential regulatory phosphorylation site in myomesin., EMBO J. 16 (1997) 211–20. doi:10.1093/emboj/16.2.211.

[9] T. Sadikot, C.R. Hammond, M.B. Ferrari, Distinct roles for telethonin N-versus C-terminus in sarcomere assembly and maintenance, Dev. Dyn. 239 (2010) 1124–1135. doi:10.1002/dvdy.22263.

[10] X. Huang, J. Li, D. Foster, S.L. Lemanski, D.K. Dube, C. Zhang, L.F. Lemanski, Protein kinase C-mediated desmin phosphorylation is related to myofibril disarray in cardiomyopathic hamster heart., Exp. Biol. Med. (Maywood). 227 (2002) 1039–46.

[11] R.K. Sihag, M. Inagaki, T. Yamaguchi, T.B. Shea, H.C. Pant, Role of phosphorylation on the structural dynamics and function of types III and IV intermediate filaments, Exp. Cell Res. 313 (2007) 2098–2109. doi:10.1016/j.yexcr.2007.04.010.

[12] Q. Zeidan, G.W. Hart, The intersections between O-GlcNAcylation and phosphorylation: implications for multiple signaling pathways., J. Cell Sci. 123 (2010) 13–22. doi:10.1242/jcs.053678.

[13] S. Mishra, S.R. Ande, N.W. Salter, O-GlcNAc modification: why so intimately associated with phosphorylation?, Cell Commun. Signal. 9 (2011) 1. doi:10.1186/1478-811X-9-1.

[14] G.W. Hart, C. Slawson, G. Ramirez-Correa, O. Lagerlof, Cross talk between O-GlcNAcylation and phosphorylation: roles in signaling, transcription, and chronic disease., Annu. Rev. Biochem. 80 (2011) 825–858. doi:10.1146/annurev-biochem-060608-102511.

[15] C.R. Torres, G.W. Hart, Topography and polypeptide distribution of terminal N-acetylglucosamine residues on the surfaces of intact lymphocytes. Evidence for O-linked GlcNAc, J. Biol. Chem. 259 (1984) 3308–3317.

[16] G. Hart, M. Housley, C. Slawson, Cycling of O-linked β-N-acetylglucosamine on nucleocytoplasmic proteins, Nature. 446 (2007) 1017–1022. doi:10.1038/nature05815.

[17] Y. Gu, S.R. Ande, S. Mishra, Altered O-GlcNAc modification and phosphorylation of mitochondrial proteins in myoblast cells exposed to high glucose., Arch. Biochem. Biophys. 505 (2011) 98–104. doi:10.1016/j.abb.2010.09.024.

[18] R.S. Haltiwanger, G.D. Holt, G.W. Hart, Enzymatic addition of O-GlcNAc to Nuclear and Cytoplasmic Proteins, J. Biol. Chem. 265 (1990) 2563–2568.

[19] J. a Hanover, M.W. Krause, D.C. Love, The hexosamine signaling pathway: O-GlcNAc cycling in feast or famine., Biochim. Biophys. Acta. 1800 (2010) 80–95. doi:10.1016/j.bbagen.2009.07.017.

[20] D.L. Dong, G.W. Hart, Purification and characterization of an O-GlcNAc selective N-acetyl-beta-D-glucosaminidase from rat spleen cytosol., J. Biol. Chem. 269 (1994) 19321–19330.

[21] Y. Akimoto, Y. Miura, T. Toda, M. a Wolfert, L. Wells, G.-J. Boons, G.W. Hart, T. Endo, H. Kawakami, Morphological changes in diabetic kidney are associated with increased O-GlcNAcylation of cytoskeletal proteins including α-actinin 4., Clin. Proteomics. 8 (2011) 15. doi:10.1186/1559-0275-8-15.

[22] C. Slawson, G.W. Hart, O-GlcNAc signalling : implications for cancer cell biology, Nature Reviews Cancer. 11 (2012) 678–684. doi:10.1038/nrc3114.

[23] Y. Fardini, V. Dehennaut, T. Lefebvre, T. Issad, O-GlcNAcylation: A new cancer hallmark?, Front. Endocrinol. (Lausanne). 4 (2013) 1–14. doi:10.3389/fendo.2013.00099.

[24] B. Lazarus, D. Love, J. Hanover, O-GlcNAc cycling: implications for neurodegenerative disorders, … J. Biochem. Cell Biol. 41 (2009) 2134–2146. doi:10.1016/j.biocel.2009.03.008.O-GlcNAc.

[25] S. Förster, A.S. Welleford, J.C. Triplett, R. Sultana, B. Schmitz, D.A. Butterfield, Increased O-GlcNAc levels correlate with decreased O-GlcNAcase levels in Alzheimer disease brain, Biochim. Biophys. Acta - Mol. Basis Dis. 1842 (2014) 1333–1339.

doi:10.1016/j.bbadis.2014.05.014.

[26] G. a Ngoh, H.T. Facundo, A. Zafir, S.P. Jones, O-GlcNAc signaling in the cardiovascular system., Circ. Res. 107 (2010) 171–85. doi:10.1161/CIRCRESAHA.110.224675.

[27] S. Dassanayaka, S.P. Jones, O-GlcNAc and the cardiovascular system, Pharmacol. Ther. 142 (2014) 62–71. doi:10.1016/j.pharmthera.2013.11.005.

[28] C. Cieniewski-Bernard, Y. Mounier, J.-C. Michalski, B. Bastide, O-GlcNAc level variations are associated with the development of skeletal muscle atrophy., J. Appl. Physiol. 100 (2006) 1499–1505. doi:10.1152/japplphysiol.00865.2005.

[29] P. Huang, S.-R. Ho, K. Wang, B.C. Roessler, F. Zhang, Y. Hu, D.B. Bowe, J.E. Kudlow, A.J. Paterson, Muscle-specific overexpression of NCOATGK, splice variant of O-GlcNAcase, induces skeletal muscle atrophy., Am. J. Physiol. Cell Physiol. 300 (2011) C456–65. doi:10.1152/ajpcell.00124.2010.

[30] S. Nakamura, S. Nakano, M. Nishii, S. Kaneko, H. Kusaka, Localization of O-GlcNAc-modified proteins in neuromuscular diseases., Med. Mol. Morphol. 45 (2012) 86–90. doi:10.1007/s00795-011-0542-7.

[31] L. Stevens, B. Bastide, J. Hedou, C. Cieniewski-Bernard, V. Montel, L. Cochon, E. Dupont, Y. Mounier, Potential regulation of human muscle plasticity by MLC2 post-translational modifications during bed rest and countermeasures, Arch. Biochem. Biophys. 540 (2013) 125–132. doi:10.1016/j.abb.2013.10.016.

[32] C. Cieniewski-Bernard, M. Lambert, E. Dupont, V. Montel, L. Stevens, B. Bastide, O-GlcNAcylation, contractile protein modifications and calcium affinity in skeletal muscle, Front. Physiol. 5 (2014) 1–7. doi:10.3389/fphys.2014.00421.

[33] C. Cieniewski-Bernard, E. Dupont, E. Richard, B. Bastide, Phospho-GlcNAc modulation of slow MLC2 during soleus atrophy through a multienzymatic and sarcomeric complex, Pflügers Arch. - Eur. J. Physiol. 466 (2014) 2139–2151. doi:10.1007/s00424-014-1453-y.

[34] J. Hedou, C. Cieniewski-Bernard, Y. Leroy, J.-C. Michalski, Y. Mounier, B. Bastide, O-linked N-acetylglucosaminylation is involved in the Ca2+ activation properties of rat skeletal muscle., J. Biol. Chem. 282 (2007) 10360–9. doi:10.1074/jbc.M606787200.

[35] C. Cieniewski-Bernard, V. Montel, S. Berthoin, B. Bastide, Increasing O-GlcNAcylation level on organ culture of soleus modulates the calcium activation parameters of muscle fibers., PLoS One. 7 (2012) e48218. doi:10.1371/journal.pone.0048218.

[36] C. Cieniewski-Bernard, B. Bastide, T. Lefebvre, J. Lemoine, Y. Mounier, J.-C. Michalski, Identification of O-linked N-acetylglucosamine proteins in rat skeletal muscle using two-dimensional gel electrophoresis and mass spectrometry., Mol. Cell. Proteomics. 3 (2004) 577–85. doi:10.1074/mcp.M400024-MCP200.

[37] C. Cieniewski-Bernard, V. Montel, L. Stevens, B. Bastide, O-GlcNAcylation, an original modulator of contractile activity in striated muscle., J. Muscle Res. Cell Motil. 30 (2009) 281–7. doi:10.1007/s10974-010-9201-1.

[38] M.C. Leung, P.G. Hitchen, D.G. Ward, A.E. Messer, S.B. Marston, Z-band alternatively spliced PDZ motif protein (ZASP) is the major o-linked beta-N-acetylglucosamine-substituted protein in human heart myofibrils, J. Biol. Chem. 288 (2013) 4891–4898. doi:10.1074/jbc.M112.410316.

[39] J. Hédou, B. Bastide, A. Page, J.-C. Michalski, W. Morelle, Mapping of O-linked beta-N-acetylglucosamine modification sites in key contractile proteins of rat skeletal muscle., Proteomics. 9 (2009) 2139–48. doi:10.1002/pmic.200800617.

[40] A.M. Farach, D.S. Galileo, O-GlcNAc modification of radial glial vimentin filaments in the developing chick brain., Brain Cell Biol. 36 (2008) 191–202. doi:10.1007/s11068-008-9036-5.

[41] C. Slawson, T. Lakshmanan, S. Knapp, G.W. Hart, A mitotic GlcNAcylation/phosphorylation signaling complex alters the posttranslational state of the cytoskeletal protein vimentin., Mol. Biol. Cell. 19 (2008) 4130–40. doi:10.1091/mbc.E07-11-1146.

[42] H. Ise, S. Kobayashi, M. Goto, T. Sato, M. Kawakubo, M. Takahashi, U. Ikeda, T. Akaike, Vimentin and desmin possess GlcNAc-binding lectin-like properties on cell surfaces., Glycobiology. 20 (2010) 843–64. doi:10.1093/glycob/cwq039.

[43] N.E. Zachara, K. Vosseller, G.W. Hart, Detection and analysis of proteins modified by O-linked N-acetylglucosamine., Curr. Protoc. Protein Sci. Chapter 12 (2011) Unit12.8. doi:10.1002/0471140864.ps1208s66.

[44] S.A. Yuzwa, M.S. Macauley, J.E. Heinonen, X. Shan, R.J. Dennis, Y. He, G.E. Whitworth, K.A. Stubbs, E.J. McEachern, G.J. Davies, D.J. Vocadlo, A potent mechanism-inspired O-GlcNAcase inhibitor that blocks phosphorylation of tau in vivo., Nat. Chem. Biol. 4 (2008) 483–90. doi:10.1038/nchembio.96.

[45] X. Yin, F. Cuello, U. Mayr, Z. Hao, M. Hornshaw, E. Ehler, M. Avkiran, M. Mayr, Proteomics analysis of the cardiac myofilament subproteome reveals dynamic alterations in phosphatase subunit distribution., Mol. Cell. Proteomics. 9 (2010) 497–509. doi:10.1074/mcp.M900275-MCP200.

[46] W.W.A. Schamel, Two-dimensional blue native polyacrylamide gel electrophoresis., Curr. Protoc. Cell Biol. Chapter 6 (2008) Unit 6.10. doi:10.1002/0471143030.cb0610s38.

[47] T. Dráb, J. Kračmerová, I. Tichá, E. Hanzlíková, M. Tichá, J. Liberda, Native polyacrylamide electrophoresis in the presence of Ponceau Red to study oligomeric states of protein complexes, J. Sep. Sci. 34 (2011) 1692–1695. doi:10.1002/jssc.201000869.

[48] S. Burattini, R. Ferri, M. Battistelli, R. Curci, F. Luchetti, E. Falcieri, C2C12 murine myoblasts as a model of skeletal muscle development: Morpho-functional characterization, Eur. J. Histochem. 48 (2004) 223–233. doi:10.4081/891.

[49] H.S. Kim, E.M. Kim, J. Lee, W.H. Yang, T.Y. Park, Y.M. Kim, J.W. Cho, Heat shock protein 60 modified with O-linked N-acetylglucosamine is involved in pancreatic β-cell death under hyperglycemic conditions, FEBS Lett. 580 (2006) 2311–2316. doi:10.1016/j.febslet.2006.03.043.

[50] J.L. Elliott, M. Der Perng, A.R. Prescott, K. a Jansen, G.H. Koenderink, R. a Quinlan, The specificity of the interaction between αB-crystallin and desmin filaments and its impact on filament aggregation and cell viability., Philos. Trans. R. Soc. Lond. B. Biol. Sci. 368 (2013) 20120375. doi:10.1098/rstb.2012.0375.

[51] R.M. Lovering, A. O'Neill, J.M. Muriel, B.L. Prosser, J. Strong, R.J. Bloch, Physiology, structure, and susceptibility to injury of skeletal muscle in mice lacking keratin 19-based and desmin-based intermediate filaments., Am. J. Physiol. Cell Physiol. 300 (2011) C803–C813. doi:10.1152/ajpcell.00394.2010.

[52] C.C. Witt, C. Burkart, D. Labeit, M. McNabb, Y. Wu, H. Granzier, S. Labeit, Nebulin regulates thin filament length, contractility, and Z-disk structure in vivo., EMBO J. 25 (2006) 3843–3855. doi:10.1038/sj.emboj.7601242.

[53] P. Tonino, C.T. Pappas, B.D. Hudson, S. Labeit, C.C. Gregorio, H. Granzier, Reduced myofibrillar connectivity and increased Z-disk width in nebulin-deficient skeletal muscle., J. Cell Sci. 123 (2010) 384–391. doi:10.1242/jcs.042234.

[54] H.L. Granzier, K.R. Hutchinson, P. Tonino, M. Methawasin, F.W. Li, R.E. Slater, M.M. Bull, C. Saripalli, C.T. Pappas, C.C. Gregorio, J.E. Smith, Deleting titin's I-band/A-band junction reveals critical roles for titin in biomechanical sensing and cardiac function, Proc. Natl. Acad. Sci. 111 (2014) 14589–14594. doi:10.1073/pnas.1411493111.

[55] J. Udaka, S. Ohmori, T. Terui, I. Ohtsuki, S. Ishiwata, S. Kurihara, N. Fukuda, Disuse-induced preferential loss of the giant protein titin depresses muscle performance via abnormal sarcomeric organization., J. Gen. Physiol. 131 (2008) 33–41. doi:10.1085/jgp.200709888.

[56] C. Butkinaree, K. Park, G.W. Hart, O-linked β-N-acetylglucosamine (O-GlcNAc): Extensive crosstalk with phosphorylation to regulate signaling and transcription in response to nutrients and stress, Biochim. Biophys. Acta - Gen. Subj. 1800 (2010) 96–106. doi:10.1016/j.bbagen.2009.07.018.

[57] P. Mamczur, D. Rakus, A. Gizak, D. Dus, A. Dzugaj, The effect of calcium ions on subcellular localization of aldolase-FBPase complex in skeletal muscle., FEBS Lett. 579 (2005) 1607–12. doi:10.1016/j.febslet.2005.01.071.

[58] J.M. Sanger, J.W. Sanger, The dynamic Z bands of striated muscle cells., Sci. Signal. 1 (2008) pe37. doi:10.1126/scisignal.132pe37.

[59] G.A. Ramirez-Correa, J. MA, C. Slawson, Q. Zeidan, N.S. Lugo-Fagundo, M. Xu, X. Shen, W.D. Gao, V. Caceres, K. Chakir, A.M. Murphy, Removal of Abnormal Myofilament O-GlcNAcylation Restores Ca2+ Sensitivity in Diabetic Cardiac Muscle, Diabetes. 64 (2015) 3573–87. doi: 10.2337/db14-1107

[60] B. Sjöblom, a. Salmazo, K. Djinović-Carugo, α-Actinin structure and regulation, Cell. Mol. Life Sci. 65 (2008) 2688–2701. doi:10.1007/s00018-008-8080-8.

[61] E. de A. Ribeiro, N. Pinotsis, A. Ghisleni, A. Salmazo, P.V. Konarev, J. Kostan, B. Sjöblom, C. Schreiner, A.A. Polyansky, E.A. Gkougkoulia, M.R. Holt, F.L. Aachmann, B. Žagrović, E. Bordignon, K.F. Pirker, D.I. Svergun, M. Gautel, K. Djinović-Carugo, The

Structure and Regulation of Human Muscle α-Actinin, Cell. 159 (2014) 1447–1460. doi:10.1016/j.cell.2014.10.056.

[62] L. Huang, T.Y.W. Wong, R.C.C. Lin, H. Furthmayr, Replacement of threonine 558, a critical site of phosphorylation of moesin in vivo, with aspartate activates F-actin binding of moesin: Regulation by conformational change, J. Biol. Chem. 274 (1999) 12803–12810. doi:10.1074/jbc.274.18.12803.

[63] Q. Huang, Ezrin/Radixin/Moesin Proteins in the Development of Diabetes and its Cardiovascular Complications, J. Diabetes Metab. 01 (2012). doi:10.4172/2155-6156.S4-005.

[64] D. Paulin, Z. Li, Desmin: a major intermediate filament protein essential for the structural integrity and function of muscle., Exp. Cell Res. 301 (2004) 1–7. doi:10.1016/j.yexcr.2004.08.004.

[65] Y. Capetanaki, R.J. Bloch, A. Kouloumenta, M. Mavroidis, S. Psarras, Muscle intermediate filaments and their links to membranes and membranous organelles, Exp. Cell Res. 313 (2007) 2063–2076. doi:10.1016/j.yexcr.2007.03.033.

[66] H. Herrmann, U. Aebi, Intermediate filaments and their associates: Multi-talented structural elements specifying cytoarchitecture and cytodynamics, Curr. Opin. Cell Biol. 12 (2000) 79–90. doi:10.1016/S0955-0674(99)00060-5.

[67] D.L. Winter, D. Paulin, M. Mericskay, Z. Li, Posttranslational modifications of desmin and their implication in biological processes and pathologies, Histochem. Cell Biol. 141 (2014) 1–16. doi:10.1007/s00418-013-1148-z.

[68] N.T Snider, M.B Omary, Post-translational modifications of intermediate filament proteins: mechanisms and functions, Nat Rev Mol Cell Biol. 15(3) (2014) 163–177. doi:10.1038/nrm3753.

[69] B. Srikanth, M.M. Vaidya, R.D. Kalraiya, O-GlcNAcylation determines the solubility, filament organization, and stability of keratins 8 and 18, J. Biol. Chem. 285 (2010) 34062–34071. doi:10.1074/jbc.M109.098996.

[70] S. Ji, J.G. Kang, S.Y. Park, J. Lee, Y.J. Oh, J.W. Cho, O-GlcNAcylation of tubulin inhibits its polymerization, Amino Acids. 40 (2011) 809–818. doi:10.1007/s00726-010-0698-9.

[71] F. Kawano, R. Fujita, N. Nakai, M. Terada, T. Ohira, Y. Ohira, HSP25 can modulate myofibrillar desmin cytoskeleton following the phosphorylation at Ser15 in rat soleus muscle, J. Appl. Physiol. 112 (2012) 176–186. doi:10.1152/japplphysiol.00783.2011.

[72] K. Hnia, C. Ramspacher, J. Vermot, J. Laporte, Desmin in muscle and associated diseases: beyond the structural function, Cell Tissue Res. 49 (2014). doi:10.1007/s00441-014-2016-4.

[73] V. Krishnamoorthy, A.J. Donofrio, J.L. Martin, O-GlcNAcylation of alphab-crystallin regulates its stress-induced translocation and cytoprotection, Mol. Cell. Biochem. 379 (2013) 59–68. doi:10.1007/s11010-013-1627-5.

[74] S. a. Houck, A. Landsbury, J.I. Clark, R. a. Quinlan, Multiple sites in alphaB-crystallin modulate its interactions with desmin filaments assembled in vitro, PLoS One. 6 (2011). doi:10.1371/journal.pone.0025859.

[75] D. Selcen, Myofibrillar myopathies., Neuromuscul. Disord. 21 (2011) 161–71. doi:10.1016/j.nmd.2010.12.007.

[76] R. Knöll, B. Buyandelger, M. Lab, The sarcomeric Z-disc and Z-discopathies., J. Biomed. Biotechnol. 2011 (2011) 569628. doi:10.1155/2011/569628.

[77] G.A. Ramirez-Correa, W. Jin, Z. Wang, X. Zhong, W.D. Gao, W.B. Dias, C. Vecoli, G.W. Hart, A.M. Murphy, O-linked GlcNAc modification of cardiac myofilament proteins: A novel regulator of myocardial contractile function, Circ. Res. 103 (2008) 1354–1358. doi:10.1161/CIRCRESAHA.108.184978.

TABLE 1. Short list of identified proteins within modulated protein complexes though O-GlcNAc level variations on RN-PAGE, by Nano-LC MS/MS: candidate proteins to explain the sarcomeric organization changes.

Protein identifications were detailed using the protein name, the UniProtKB accession number, the predicted MW (Molecular Weight), the sequence coverage, the number of identified peptides. Mascot score was obtained from Mascot database (www.matrixscience.com). Bands numbers were assigned to the identified proteins from the RN-PAGE on figure 3.

Protein name	Accession no. (UniProtKB)	Predicted MW (kDa)	Sequence coverage (%)	No. of identified peptides	Mascot score	Band
Filamin-C	Q8VHX6	290.9	22	35	2431	1-2
Moesin	P26041	67.7	11	6	407	1-2-3
Desmin	P31001	53.5	16	4	326	1-2-3
Alpha-crystallin B chain	P05811	20.1	28	4	265	1-2-3
Alpha-actinin-1	Q7TPR4	103	6	4	141	3

FIGURES LEGEND

FIGURE 1. Quantification of the global O-GlcNAcylation level in C2C12 myotubes by western blot.

Proteins from (A) whole cellular extract and (B) myofilament-enriched fraction were separated on 7.5% Stain-free gel. Whole proteins profiles corresponding to stain-free images were presented above, while the western blot using RL-2 antibody were presented below. For Thiamet-G treatments and reversions (Rev.), histograms corresponding to the variation of the relative O-GlcNAc level were presented at the bottom of figure. RL2 signal values were normalized to stain-free signal, an internal standard and to respective control. Data were expressed as mean ± SEM and were representative of n = 9 (from N = 3 independent cell cultures) for each group. Significant differences compared to their respective control (*) or between groups (* above a horizontal bar) were referred as follows: *p<0.05; **p<0.01; ***p<0.001 (Mann-Whitney test).

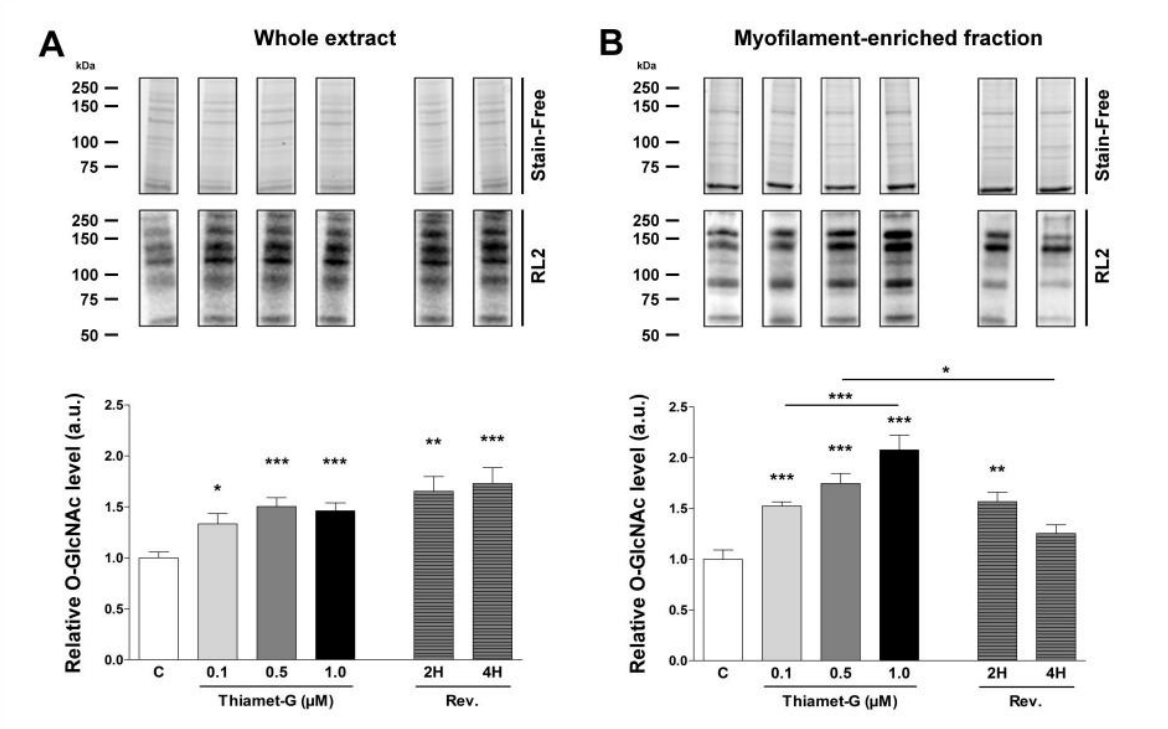

FIGURE 2. Changes of the sarcomere morphometry depending on the variations of the global O-GlcNAc level in the myofilament-enriched fraction.

(A) MHC striations (Alexa Fluor 555, in red) and nucleus (DAPI, in blue), were visualized by confocal microscopy. (B) Four morphometric parameters of the sarcomere were determined: the dark band (green), the M-line (blue) and I-band widths (purple) and the sarcomere length (red). (C) Depending on the O-GlcNAc level variations in the myofilament-enriched fraction quantified in figure 1, morphometric measurements were carried out, and represented by curves on the graphs. n = 70 measurements were determined per parameter (from N = 3 independent cell cultures). Data were expressed as mean ± SEM. Significant differences compared to control (represented by the vertical dotted line on graphs) were referred as follows: *$p<0.05$; **$p<0.01$; ***$p<0.001$ (t-test). (D) The summary diagram of the sarcomere stressed on the changes in sarcomere organization due to the variations of the global O-GlcNAc level.

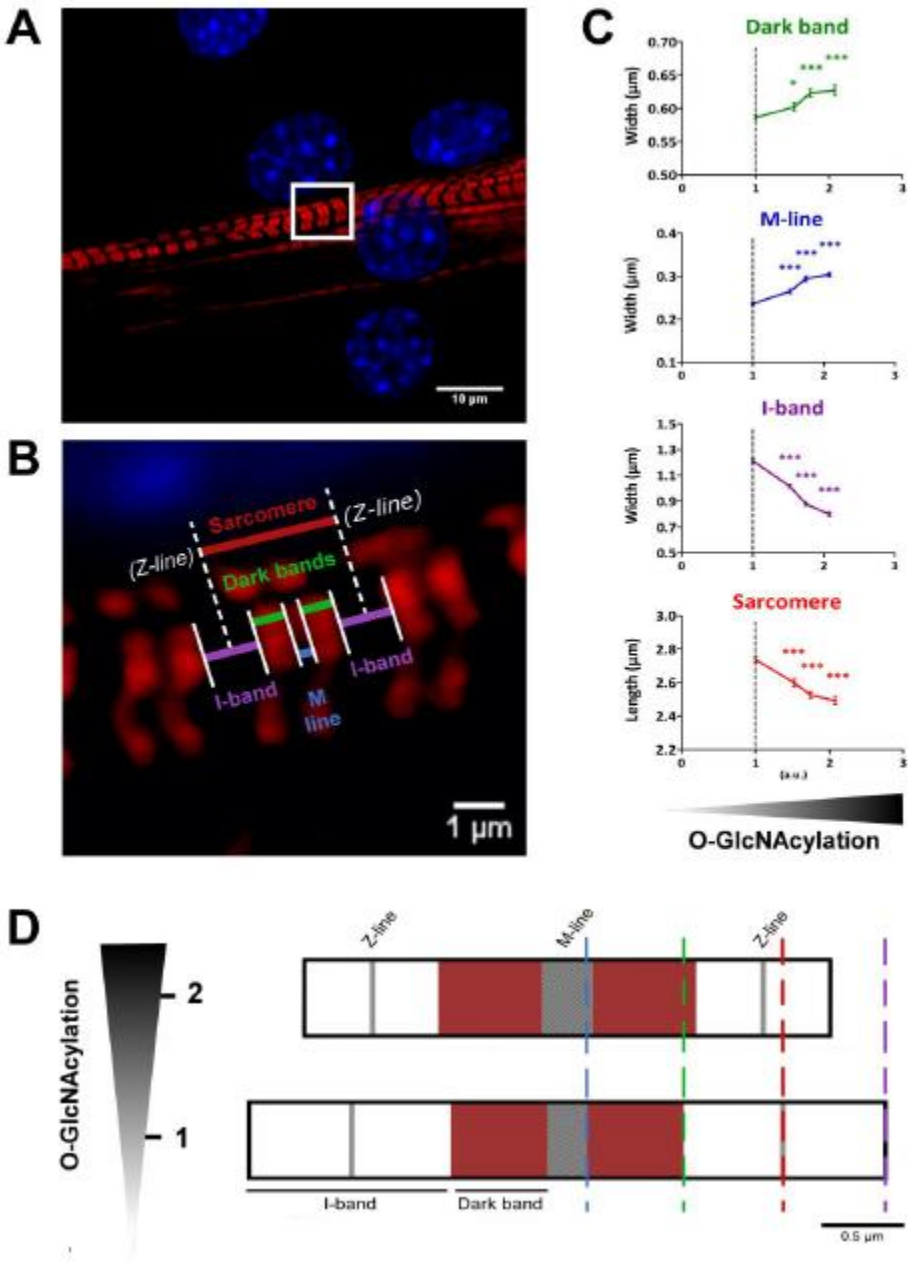

FIGURE 3. Modulation of some protein complexes by using Red-Native PAGE.

Native proteins were separated on 5% native polyacrylamide gel containing Red Ponceau S. Gel was then colloidal-blue stained. Results from Thiamet-G treatments for 4 hours (at 0.1 and 0.5 µM) and its control were represented. The differential proteins regions compared to control were characterized by vertical lanes, then enlarged at the right side of the figure, and numbered. Experiment was performed three times.

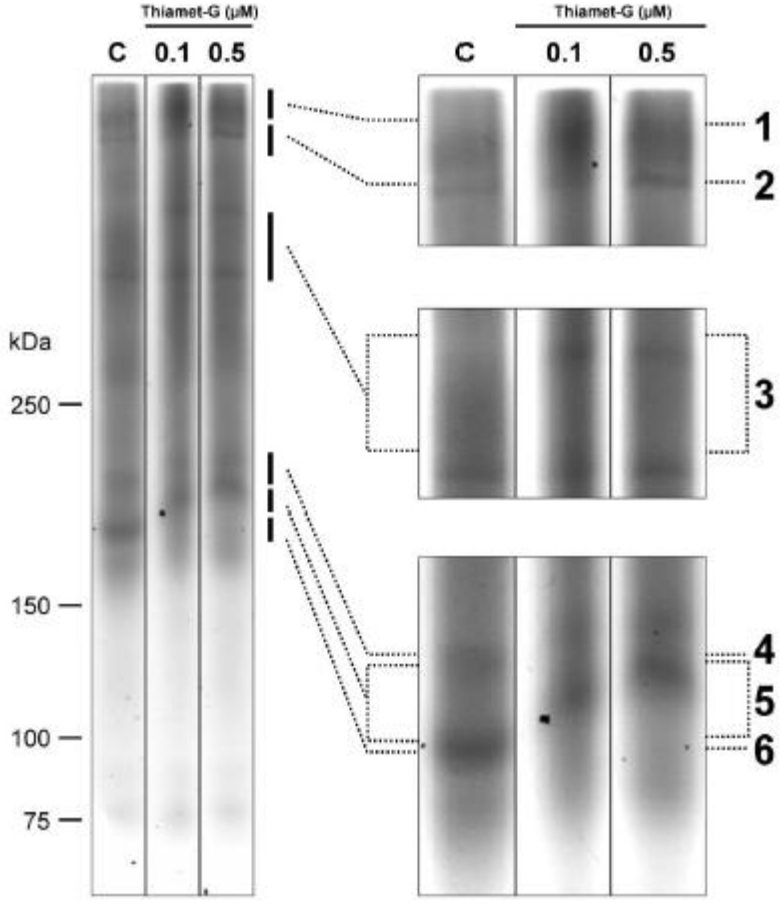

FIGURE 4. The structural proteins desmin, αB-crystallin, α-actinin, filamin-C and moesin belong to the complexes modulated consecutively to the global O-GlcNAcylation variations. From native proteins (A), non-retained fraction of desmin (B), αB-crystallin (C), α-actinin (D), filamin-C (E), moesin (F) after co-immunoprecipitation of these proteins of interest were separated using the RN-PAGE protocol. Gel was then colloidal-blue stained. The empty arrows correspond to IgG bands. The full arrows indicated changes of complexes profile compared to the native protein extract (A).

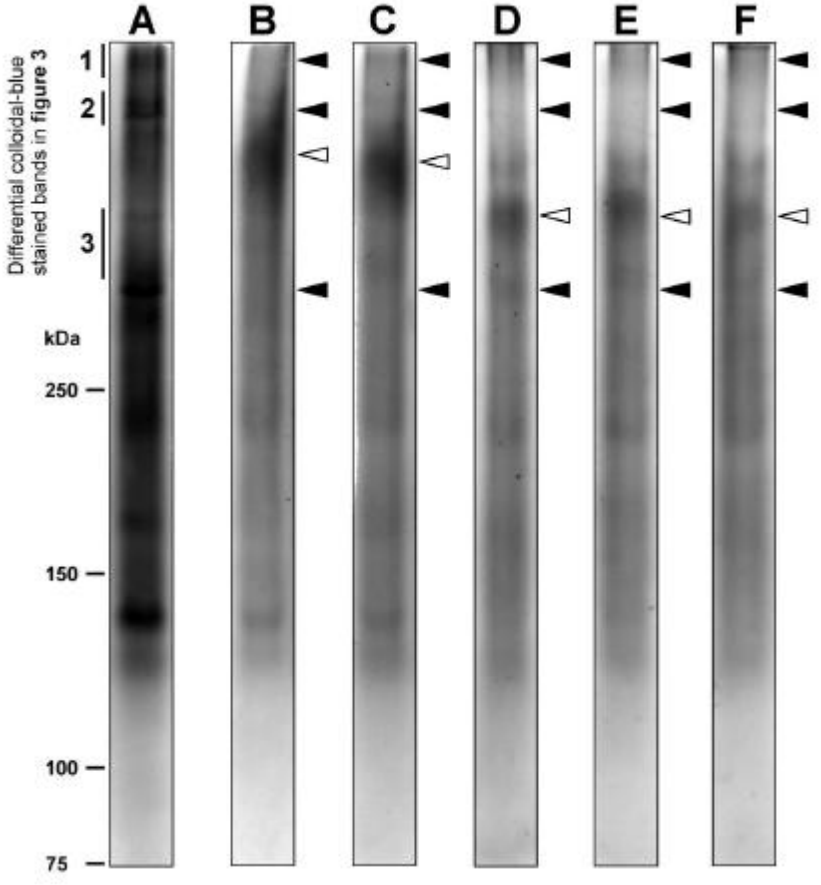

FIGURE 5. O-GlcNAcylation level of some candidate proteins according to pharmacological treatments.

The O-GlcNAcylated proteins of whole extract were enriched using RL2 immunoprecipitation protocol. The separation of immunoprecipitated proteins on 8-16% stain-free SDS-PAGE was followed by a western blot analysis using antibodies directed against filamin-C (A), αB-crystallin (B), and desmin (C). Results from Thiamet-G (TMG) treatment (at 0.5 µM) and its control were represented. Western blot images were presented at the top of the figures. Signal intensity was normalized to IgG band intensity (not shown) and to control. Results were presented on histogram at the bottom of the figures. Data were expressed as mean ± SEM and were representative of n = 9 (from N = 3 independent cell cultures) for each group. Significant differences compared to their respective control were referred as follows: *p<0.05 (Mann-Whitney test).

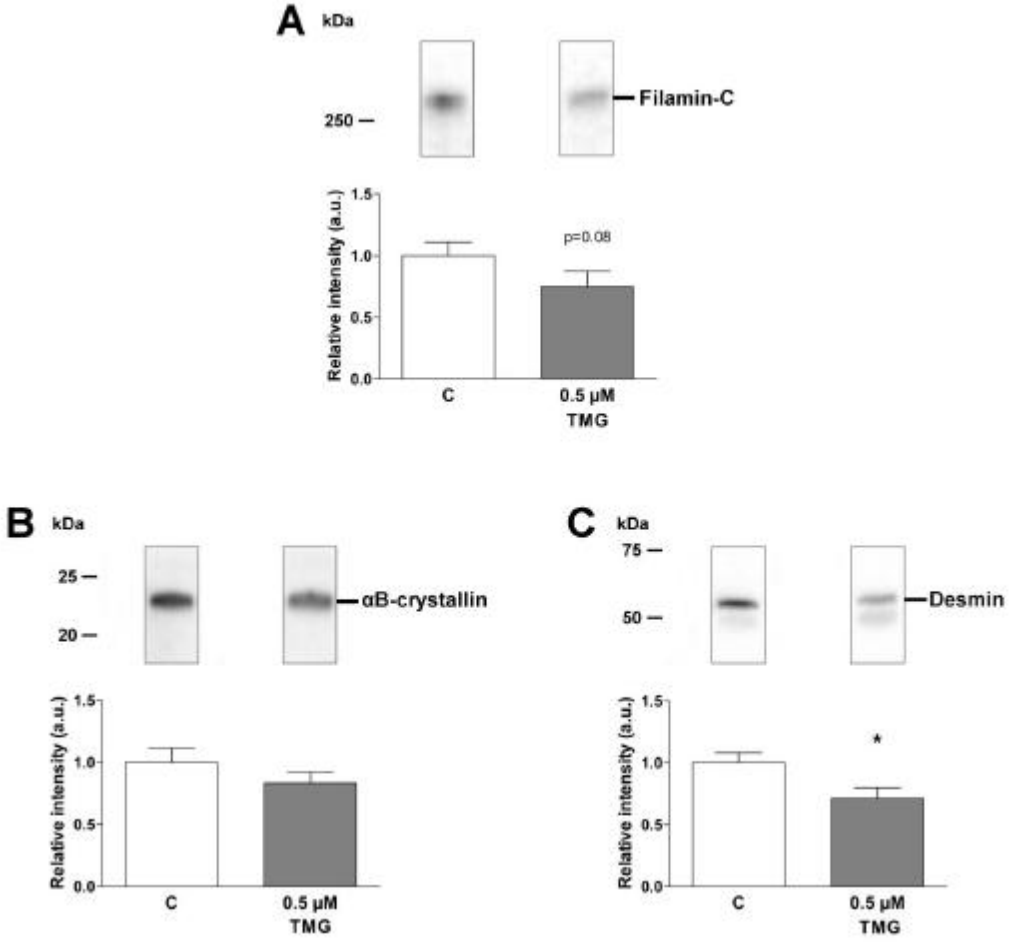

FIGURE 6. Protein interactions of some candidate proteins were modulated though global O-GlcNAcylation variations.

Native proteins were separated on 5% Red-Native PAGE. Proteins were then transferred and analyzed on desmin (A), αB-crystallin (B), α-actinin (C), moesin (D) and filamin-C (E) western blot. Quantification of signals from Thiamet-G (TMG) treatment (at 0.5 µM) and its control were represented. Western blot images and profile lanes (in red) were presented at the left of the figures; protein bands have been described and numbered. Protein expression of the numbered band in bold with an ***** was quantified and normalized to control; results were presented on histogram at the right side of the figures. Then, proteins of whole cellular extracts were separated on 8-16% linear gradient stain-free SDS-PAGE, transferred and analyzed on desmin (F), αB-crystallin (G), α-actinin (H), moesin (I) and filamin-C (J) western blot. Western blot images were presented at the top of the figures. Respective signal intensity was normalized to total protein (stain-free signal described in figure 1), to control and to an internal standard; results were presented on histogram at the bottom of the figures. Data were expressed as mean ± SEM and were representative of n = 9 (from N = 3 independent cell cultures) for each group. Significant differences compared to their respective control were referred as follows: *$p<0.05$; **$p<0.01$ (Mann-Whitney test).

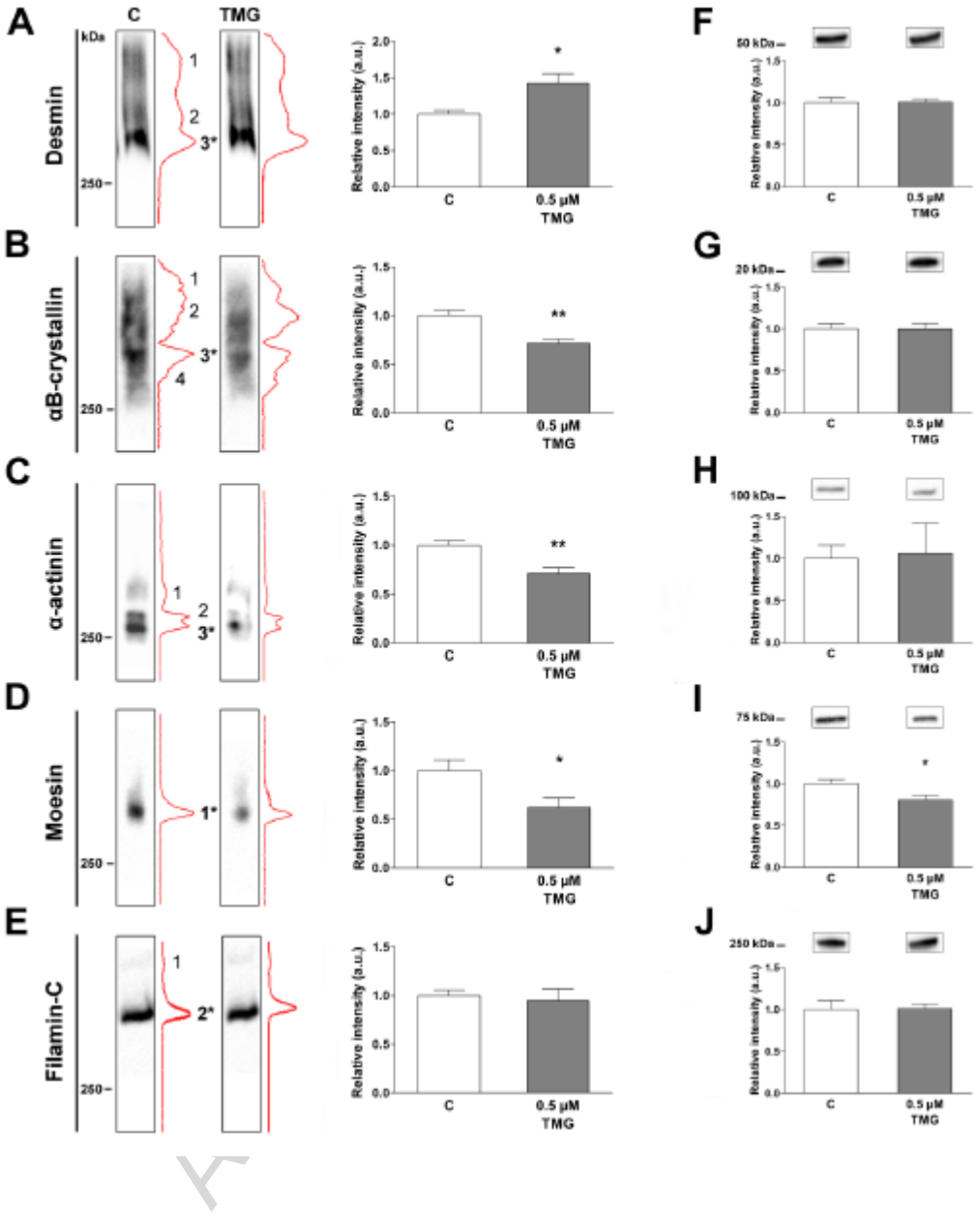

FIGURE 7. Protein interactions between desmin and αB-crystallin were modulated though global O-GlcNAcylation variations.

Co-immunoprecipitation (Co-IP) of αB-crystallin (A) and desmin (B) were performed, followed by electrophoretic separation on stain-free SDS-PAGE, and immunodetection of αB-crystallin and desmin using western blot for each co-IP. Results from Thiamet-G (TMG) treatment (at 0.5 µM) and its control were represented. Western blot images were presented at the top of the figures. (A) Desmin signal intensity was normalized to αB-crystallin signal and control. (B) αB-crystallin signal intensity was normalized to desmin signal and control. Results were presented on histogram at the bottom of the figures. Data were expressed as mean ± SEM and were representative of n = 12 (from N = 3 independent cell cultures) for each group. Significant differences compared to their respective control were referred as follows: *p<0.05 (Mann-Whitney test).

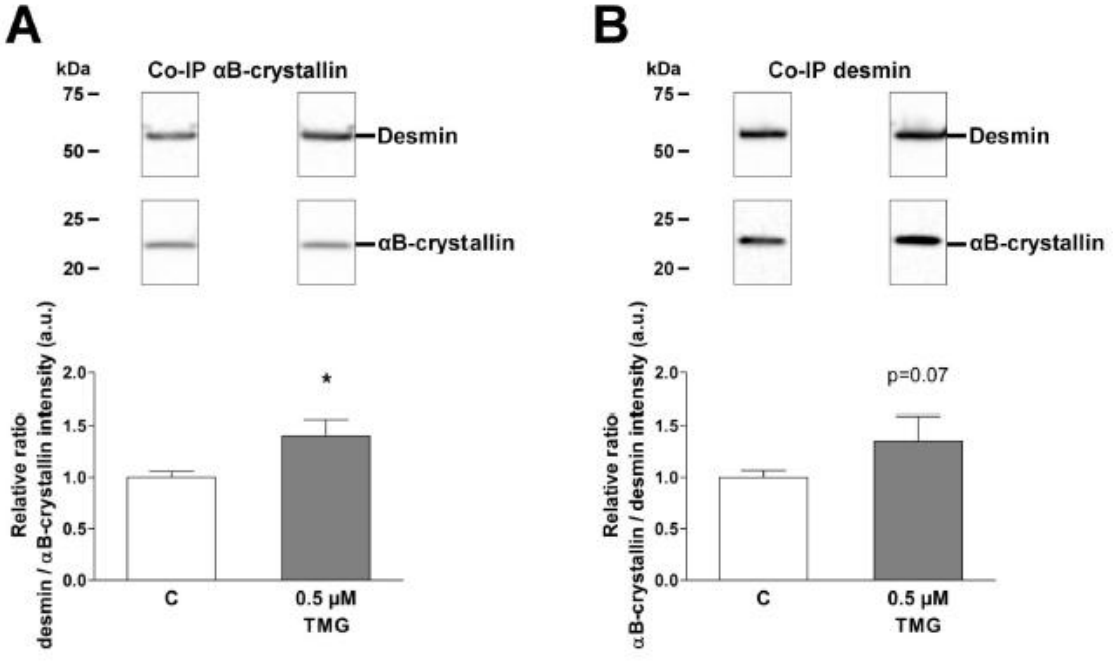

FIGURE 8. Simplified interactome of « candidate proteins » that could explain the modulation of the sarcomere structure following O-GlcNAcylation variations in C2C12 myotubes.

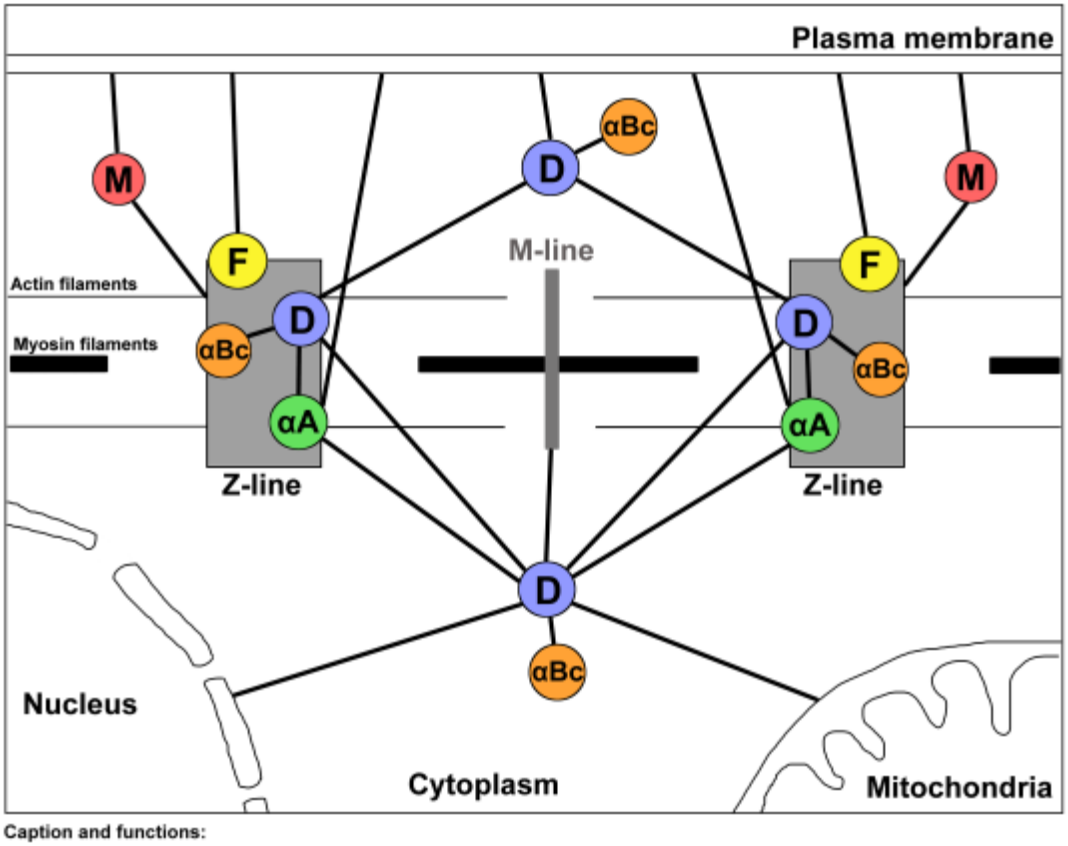

Caption and functions:

Protein-protein interactions

D **Desmin** - This intermediate filament forms a fibrous network connecting myofibrils to each other and to the plasma membrane and organelles from the periphery of the Z-line structures. It's essential for the structural integrity of sarcomere.

αBc **αB-crystallin** - It's a small heat-shock protein and functions as a chaperone for desmin. It modulates the aggregation, polymerization and structure of desmin.

αA **α-actinin** - It is located to the Z-line of the sarcomere. It is necessary for the attachment of actin filaments to the Z-line and provides a structural link between sarcomere and plasma membrane. Sarcomeric α-actinin interacts with structural proteins and proteins involved in a variety of signaling and metabolic pathways in the Z-line.

F **Filamin-C** - It works as an actin-binding-like protein and it is involved in the reorganization of the actin cytoskeleton. It is bound to the Z-line and participates to the connection between plasma membrane and sarcomere. It displays structural functions at the Z-line and maintains the structural integrity of sarcomere.

M **Moesin** - It is a actin-binding protein. It is involved in the regulation of the cytoskeleton and could interact with the Z-line. It's a cross-linker between plasma membrane and actin.

Highlights

This paper supports the role of O-GlcNAcylation, a particular glycosylation, in the regulation of interactome, in particular the sarcomeric organization. For the first time, we demonstrated a key role of the O-GlcNAcylation in myofibrillar interactome by the modulation of protein-protein interactions between key structural proteins.

This paper will have interest for glycobiologists (through O-GlcNAcylation), for physiologists and/or cell biologists (through the sarcomeric organization), as well as for proteomists (through interactome).